

Hippocampus Segmentation using a Local Prior Model on its Boundary

Dimitrios Zarpalas, Anastasios Zafeiropoulos, Petros Daras, *Member, IEEE*, and
Nicos Maglaveras, *Senior Member, IEEE*

Abstract—Segmentation techniques based on Active Contour Models have been strongly benefited from the use of prior information during their evolution. Shape prior information is captured from a training set and is introduced in the optimization procedure to restrict the evolution into allowable shapes. In this way, the evolution converges onto regions even with weak boundaries. Although significant effort has been devoted on different ways of capturing and analyzing prior information, very little thought has been devoted on the way of combining image information with prior information. This paper focuses on a more natural way of incorporating the prior information in the level set framework. For proof of concept the method is applied on hippocampus segmentation in T1-MR images. Hippocampus segmentation is a very challenging task, due to the multivariate surrounding region and the missing boundary with the neighboring amygdala, whose intensities are identical. The proposed method, mimics the human segmentation way and thus shows enhancements in the segmentation accuracy.

Keywords—Medical imaging & processing, Brain MRI segmentation, hippocampus segmentation, hippocampus-amygdala missing boundary, weak boundary segmentation, region based segmentation, prior information, local weighting scheme in level sets, spatial distribution of labels, gradient distribution on boundary.

I. INTRODUCTION

SEGMENTATION of anatomical structures from medical images, such as MRI and CT, has found numerous applications. Current image-based diagnosis, therapy evaluation, surgical planning and navigation highly depend on the segmentation procedure. Medical expert's time though, is both limited and valuable to perform manual segmentations, which also lack reproducibility. The need for automatic segmentation in medical images and its challenging nature, are the main reasons that attract researchers on the topic.

The main challenges of the topic arise from the fact that neighboring structures share the same intensity characteristics and weak boundaries. This exactly is the case with the hippocampus and amygdala complex (Fig. 1). Evidences that alterations of hippocampus and amygdala could serve as potential biomarkers for mental diseases [13] [5], have increased the interest for automated methods that would accurately, robustly and reproducibly segment those structures.

Due to the importance of the problem and the variety of other applications, extensive study has been carried out and

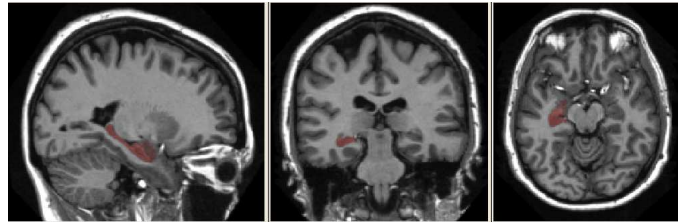


Fig. 1. MRI of a brain with highlighted the hippocampus and amygdala structures.

various methods and techniques have been proposed which are mainly based on deformable models. Active Contour Models (ACM) have been proved to be the most efficient formulation for such segmentations. ACMs try to deform a contour, by following information extracted from the given image, under some pre-defined constraints. The nature of the constraints differentiate the methods to two types: the gradient-edge based methods [2] and the region-based methods [4]. Though a hybrid model that combines them has also been proposed [18], the second type still seems to offer more solutions in the medical image domain, since it utilizes regional statistical information of the intensities to control the contour. Thus, is much less sensitive to noise and performs robustly in the case of weak and smooth edges, in contrast with the edge-based models that utilize gradient stopping functions, which by definition can not handle those cases. Due to these highly attractive properties, a lot of variations of the original region-based model have been proposed in the literature. In [8] a new variational level set formulation has been proposed that does not require re-initialization. [17] is a quite recent formulation with selective local-global behaviour in the segmentation. Those models though, solely depend on current information, i.e. the image at hand. However, in medical image analysis prior information is critical for understanding and segmentation of anatomical structures, since their shape shares common characteristics over the population.

Significant effort has been devoted on ways for capturing and analyzing shape prior information. The most common approach is to perform a statistical analysis over the distance maps of known shapes through PCA to produce a shape variational model [7]. In [6] wavelet analysis is performed on the coordinates of the structure's boundaries and the PCA analysis uses the wavelet coefficients, to overcome the problem of small training set. One of the first attempts to incorporate shape prior knowledge in the level set segmentation process was made in

Dimitrios Zarpalas, Anastasios Zafeiropoulos and Petros Daras are with the Informatics and Telematics Institute, Centre for Research and Technology Hellas, 1st km Thessaloniki-Panorama Rd, P.O. Box 60361, 57001, Thessaloniki, Greece (email: {zarpalas, zafeirop, daras}@iti.gr).

Dimitrios Zarpalas and Nicos Maglaveras (email: nicmag@med.auth.gr) are with the Laboratory of Medical Informatics, Medical School, Aristotle University of Thessaloniki, 54124 Thessaloniki, Greece.

[7], where the shape prior was attracting the evolution, at each deformation iteration, on a shape that would be acceptable to the shape prior. Since then a lot of other techniques have been proposed that try to bias the segmentation towards learned shapes [15], [3], [1].

Yang et. al in [16], moved a step further and introduced along with the shape prior, the neighborhood prior knowledge, in an effort to take advantage during the evolution information from neighboring structures. The prior knowledge was embedded into the region-based framework, by adding the prior energy term into the optimization formulation. The way though, that the two energy terms are merged, does not take full advantage of the prior knowledge, as they are merged through a global weighting scheme. The hippocampus boundary suffers from missing boundaries mainly in the borders with amygdala. In most of the rest boundary, evident, if not strong, gradients do exist. Why is then the prior energy term affecting the contour evolution in regions with high gradients? And why is the image term affecting the contour evolution in the borders with amygdala, though there is no practical evidence that this term would converge on the actual boundary?

Knowing, through experience, the expecting gradient values on the perimeter of the structure of interest is an excellent way to balance locally between the two energy terms. Capturing this information, forms a novel, energy blending scheme, that locally defines the expected importance of each energy term. The proposed local weighting matrix defines the extent to which one should trust the image's gray-scale information or the prior knowledge at a voxel level.

The proposed method utilizes region-based segmentation algorithms using active contours based on the level set distribution model. A prior information model is introduced, that is formulated from a labelled training set, which captures the spatial distribution of the hippocampus labels. The active contours evolve according to the image information and the prior knowledge in a single framework. Those two driving forces are combined through a novel local weighting matrix, the Gradient Distribution on Hippocampus Boundary (GDHB) map, i.e. a local weighting matrix which acts as an experienced balancer between the image and the prior information. In contrast to global multiplicative weighting factors, which act globally on the whole term, GDHB contains statistical information about the magnitude of the image gradient on the boundary of hippocampus, and thus can act on each boundary voxel independently.

In the following sections we give the necessary background on region-based segmentation with shape prior, and thoroughly explain our contributions in full exploitation of prior knowledge. Experimental results will prove the validity of the proposed method by comparison with the existing shape prior based segmentation technique.

II. LEVEL SETS WITH VARIATIONAL SHAPE PRIOR

A. Region Based Segmentation

The model, that is used for the image term of the segmentation process, is based on intensity statistical information of the inner and outer regions of the evolving contour. The average

intensities inside and outside the contour adjust the image update term in order to separate the structure of interest from the background. The model used in this work is the well know Chan-Vese framework [4], which can be seen as a special case of the Mumford-Shah [12] problem:

Let Ω denote a bounded open subset of R^2 , with $\partial\Omega$ its boundary, and $C(s) : [0, 1] \rightarrow R^2$ is a parameterized curve in Ω . The curve C can be also implicitly represented via a Lipschitz function ϕ by $C = \{(x, y) | \phi(x, y) = 0\}$. C partitions Ω into the inside C set Ω_1 in which $\phi(x, y) > 0$, and the outside C set Ω_2 in which $\phi(x, y) < 0$. For a given image I in domain Ω the Chan-Vese model is formulated by minimizing the following energy functional:

$$E_{CV} = \lambda_1 \int_{\Omega_1} |I(x, y) - c_1|^2 dx dy + \lambda_2 \int_{\Omega_2} |I(x, y) - c_2|^2 dx dy, \quad (x, y) \in \Omega \quad (1)$$

where c_1 and c_2 are the average intensities of Ω_1 and Ω_2 respectively. By minimizing equation (1), c_1 and c_2 are calculated as:

$$c_1(\phi) = \frac{\int_{\Omega} I(x, y) \cdot H_{\epsilon}(\phi) dx dy}{\int_{\Omega} H_{\epsilon}(\phi) dx dy} \quad (2)$$

$$c_2(\phi) = \frac{\int_{\Omega} I(x, y) \cdot (1 - H_{\epsilon}(\phi)) dx dy}{\int_{\Omega} (1 - H_{\epsilon}(\phi)) dx dy} \quad (3)$$

where $H_{\epsilon}(\phi)$ is the Heaviside function. Furthermore, augmenting the energy term in equation (1) with regularization terms of length and area energy terms, results to a smoother solution. By minimizing it, the corresponding variational level set formulation is obtained:

$$\frac{\partial \phi}{\partial t} = \delta_{\epsilon}(\phi) \left[\mu \operatorname{div} \left(\frac{\nabla \phi}{|\nabla \phi|} \right) - \nu - \lambda_1 (I - c_1)^2 + \lambda_2 (I - c_2)^2 \right] \quad (4)$$

where $\mu, \nu \geq 0$ control the smoothness and the evolution speed respectively, while $\lambda_1, \lambda_2 > 0$ control the image data driven force inside and outside C respectively. δ_{ϵ} denotes the Dirac function. This model has been widely used in applications that require segmentation on weak boundary objects. However, when background intensities are of similar value to that of the object to be segmented, and their regions are separated with vague boundaries (e.g. hippocampus and amygdala), the contour can leak and start expanding on the background. Due to the nature of the problem, the segmentation model by itself is not adequate to separate the hippocampal voxels from the rest of the brain structures. Figure 2(a) shows how this model fails to capture the hippocampus boundaries and how challenging the problem is.

B. Variational Shape Prior Modeling through PCA

To overcome this situation, Leventon et.al [7] proposed the use of a probabilistic shape prior model, captured from a training population through a PCA analysis. This approach was also followed by Yang et. al [16]. The difference between those two methods was that in [7] gradient based geodesic active contours (GAC) model was used, while in [16] the aforementioned Chan-Vese framework. Following the analysis in [16], after incorporating the shape prior model in the energy term, the evolution equation becomes:

$$\frac{\partial \phi}{\partial t} = \delta_{\epsilon}(\phi) \left[\mu \operatorname{div} \left(\frac{\nabla \phi}{|\nabla \phi|} \right) - \nu - \lambda [(I - c_1)^2 - (I - c_2)^2] \right] -$$

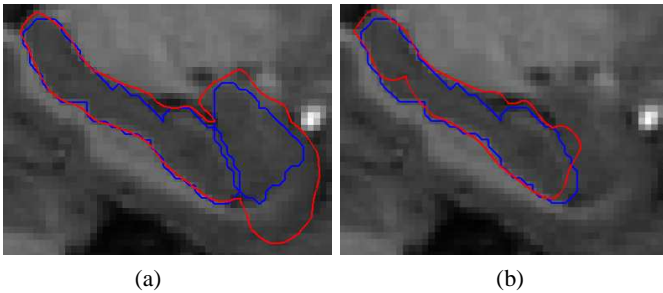


Fig. 2. (a) Segmentation outcome of the Chan-Vese model (red contour) that leaks from the hippocampus-amygdala boundary (blue contours) on a central slice of the hippocampus. (b) Segmentation outcome when variational shape prior is introduced.

$$-\omega \cdot g\{U_K \Sigma_k^{-1} U_k^T [G(\phi - \bar{\phi})]\} \quad (5)$$

where $\lambda = \lambda_1 = \lambda_2$ and ω are the two “global” weighting factors that balance between the image data term and the shape prior term. $G(\cdot)$ is an operator that generates the vector representation of a matrix by column scanning and $g(\cdot)$ the inverse operator of G . U_k , Σ_k and $\bar{\phi}$ are the k -principal component basis functions matrix, the singular values matrix and the mean shape of the training set produced by PCA, respectively.

The results using this shape prior model are promising, as can be seen in figure 2(b), but still leave enough space for more contributions.

III. PROPOSED MODEL

Incorporating prior knowledge in the segmentation procedure proved a very reasonable and successful choice. However the trade off among the two energy terms, i.e. the image data term and the shape prior term, is not straightforward and highly depends on the specific structure under investigation. Still, in all previous works, this balance is modelled through global weighting factors, which is not the way a human rater would perform the procedure. The human expert would trust the image information for the regions of the hippocampus boundary that border with the white matter, but would use his experience to trace the weak borders with amygdala. Thus, in order to model this procedure, one has to blend the two energy terms in a local fashion. This means to learn where to trust the image information, and where to neglect it and use prior information instead. This way prior knowledge is being exploited to its full extend.

However, a variational shape prior model could not be applied on a locally defined weighting scheme, since such a term tries to find the boundary with the most likely shape, describing it by a set of global coefficients (i.e. the PCA projection coefficients). Thus, the prior information that will get included in the segmentation process, should also be locally defined. The following sections describe how the local weighting scheme, called GDHB, and the prior information term are formed and incorporated in the region based segmentation framework.

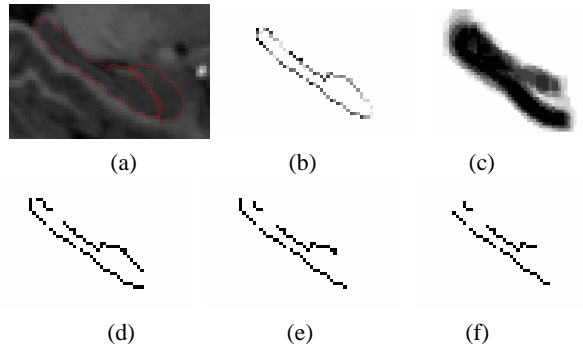


Fig. 3. Illustration of the GDHB map generation. (a) Outlines of the hippocampus and amygdala, (b) the gradient values on the boundary of hippocampus, (d)-(e)-(f) thresholding outcomes with ascending threshold values and (c) the final averaged GDHB map revealing how much the evolving contour should trust the image information and how much the prior information on every voxel.

A. Building Gradient Distribution on Hippocampus Boundaries

GDHB derives from image gradient analysis on the training set. More specifically, in each image, we isolate the hippocampus’s boundary and calculate the magnitude of the image gradient on it. Practically, low gradient magnitude values on the perimeter of the structure of interest are associated with high probability of contour leakage during the evolution process. On the other hand, higher values decrease the probability to leak from those specific boundary pixels.

A thresholding operation is performed on the gradient values, which also tries to connect neighboring pixels with similar gradient value and direction. Binarization separates the boundary to its strong and weak gradient parts. This procedure is depicted in figure 3 for various thresholds. A map is produced that shows on which parts, of this particular boundary, image information should drive the segmentation and on which the prior term should take over. In an effort to build something more generic, this information is propagated to the surrounding region, by applying morphological operations; a long and narrow structuring element, aligned for each pixel on the boundary’s normal direction, performs dilation. Hence, the values of this map represent the likelihood that an evolving contour will face regions with either strong or weak borders, while it evolves towards the boundary. The above process is repeated for each of the training images. The produced individual GDHB maps, are averaged and the final GDHB map with values in $[0, 1]$, is produced (Fig 3(c)) that contains generalized gradient distribution information of the hippocampus boundary.

B. Modeling Prior Information

In order to satisfy the constraint that the prior information should be defined locally to be applicable to the GDHB framework, a voxel-based statistical model is defined. Adopting the voxel-based context of atlas based segmentation, where an atlas image assigns a label l to each voxel v , a statistical model of spatial class label distribution is produced, over the training set. Each labelled image L_n , $n = 1, \dots, N$ is a

binary image, with $L_n(v) = 1$ for voxels v that belong to the hippocampus and 0 otherwise. In order to construct the empirical spatial distribution of labels, the N labelled images are rigidly registered based on the hippocampus and their labels' sum is averaged over the population, producing image L (see figure 4) which gives the empirical probability for every voxel $p(l_v) \in [0, 1]$ to belong to hippocampus, based on its coordinates. This image models the spatial distribution of the labels, and has higher values at voxels along the expected shape of hippocampus and lower values at distant voxels of the mean shape. When a test image is registered on the training images, it assigns to each pixel, based on its location, the probability to belong to the desired structure.

C. Incorporating Prior Information into the Segmentation Process

Proper incorporation of the prior knowledge in the level set evolution framework is obviously of critical importance. The choice of modeling the prior knowledge with the labels' distribution has a huge advantage, since it can be straightforwardly used as a second input image on the regional segmentation framework of Chan-Vese. Thus, averaging probabilities of voxels that belong inside and outside of the evolving contour. This leads to an energy minimization problem which forces the contour to evolve between regions that are more likely than others representing lower probabilities.

$$E_{PR} = v_1 \int_{\Omega_1} |L(x, y) - d_1|^2 dx dy + v_2 \int_{\Omega_2} |L(x, y) - d_2|^2 dx dy, \quad (x, y) \in \Omega \quad (6)$$

where d_1 and d_2 are now the probabilities of the regions inside and outside C and are calculated similarly with c_1 and c_2 . v_1 and v_2 correspond to λ_1 and λ_2 . Keeping v_1 and v_2 coefficients equal, forces the prior information to be equally balanced between high likely voxels (red region in Figure 4) and marginal voxels (light blue-yellow). Adjusting v_1 and v_2 balances the weight between highly probable areas and marginal areas.

Combining the two energy terms through GDHB gives the total energy to be optimized:

$$E = GDHB \cdot E_{CV} + (1 - GDHB) \cdot E_{PR} \quad (7)$$

whose update equation becomes:

$$\frac{\partial \phi}{\partial t} = \delta_\epsilon(\phi) \left[\mu \operatorname{div} \left(\frac{\nabla \phi}{|\nabla \phi|} \right) - \nu - GDHB \cdot \left(\lambda_1 (I - c_1)^2 - \lambda_2 (I - c_2)^2 \right) - (1 - GDHB) \cdot \left(v_1 (L - d_1)^2 + v_2 (L - d_2)^2 \right) \right] \quad (8)$$

Due to the nature of the labels' spatial distribution mask and the values of the GDHB, this model always converges on a boundary that is indeed near the hippocampus. The leakage phenomenon is totally diminished, since in the regions away of the hippocampus, GDHB guides the segmentation solely based on the prior information, and on those regions, the labels' spatial distribution mask points that there is zero likelihood those regions to belong to hippocampus. This leakage preventing behaviour can not be guaranteed with the variational shape prior models.

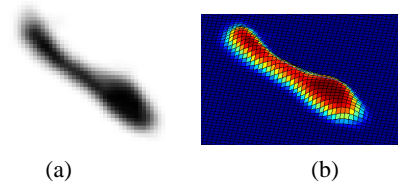


Fig. 4. Illustration of the Spatial Distribution of Hippocampal labels, as a gray scale image and as a surface.

IV. EXPERIMENTAL RESULTS

Evaluation Dataset

The proposed methodology has been tested on 13 T1 weighted MP-RAGE MR images, randomly chosen from the OASIS database [10]. All subjects in the OASIS database are healthy and right handed, of both sexes. The MR images were acquired on a 1.5-T Vision scanner. For every subject, 3-4 different MRIs were captured and the first of these was registered on the atlas space of Talairach and Tournoux [14]. The remaining scans were registered on the first one and averaged. After resampling the result is a single, high-contrast, isotropic image with 1mm voxel thickness. A professional radiologist manually traced the hippocampus volume on those 13 images, in order to build the training set. Apart of the OASIS pre-processing, the selected MR images were further rigidly registered on the hippocampus center of mass. Level set functions were used to formulate the problem and signed distance maps in order to represent the hippocampal structures. Each of the curves in the training dataset is embedded in the proposed model as the zero level set of a higher dimensional level set function.

Comparisons

The proposed algorithm was evaluated in the context of the leave-one-out procedure. For every excluded test image, a new hippocampus spatial distribution map and GDHB map was generated. For comparison purposes, results of the combined framework of Chan-Vese and variational shape prior have been calculated, which will be abbreviated as SP in the following text.

To initialize the algorithm, we took advantage of the captured prior knowledge. The seeding region was selected as the set of voxels with very high probability to belong to the hippocampus. The hippocampus spatial distribution map directly gives this information. For the SP method we followed the seeding technique of [16], where it was argued that the SP methodology is quite invariant to its initialization. Three seeds inside the body of hippocampus (in the head, in the tail and in the central area of the hippocampus) was used for initialization. However, to avoid any possible unfairness, in the following experiments the same seeding region with the proposed method was used as a second alternative for the SP method.

The advantages of using the hippocampus spatial distribution map to provide the initialization, is that it is automatic, and offers a large and very reliable seeding region along the complete body of the hippocampus. This is advantageous,

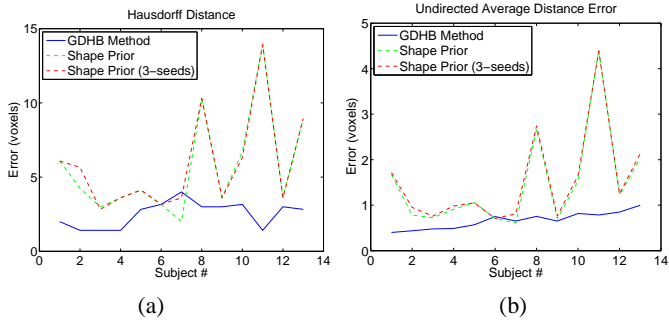


Fig. 5. Comparisons based on (a) the Hausdorff distance, and (b) the undirected averaged distance.

since larger area of initialization leads to more accurate calculation of the average intensities c_1 and c_2 and consequently to lower number of iterations to fully segment an object from the background.

The following results refer to segmentations performed on a central sagittal slice of each MRI. Performance and accuracy of the two comparing methods is evaluated through several popular metrics, i.e. the Hausdorff distance [9] in figure 5(a), the undirected averaged distance [16] in figure 5(b), precision vs recall [11] in figures 6(a),(b) and the F_b measure (Fig. 6(c)) which is a proportional combination of precision-recall measures with a weighting factor b to balance between the importance of precision vs recall. $b = 1$ assigns equal weight, and F_1 equals the Dice coefficient which measures set agreement. In terms of false positive, false negative and true positive counts, F_1 equals:

$$F_1 = \frac{2 \cdot TP}{(FP + TP) + (TP + FN)}, \quad F_1 \in [0, 1] \quad (9)$$

A value of $F_1 = 0$ indicates no overlap between the actual and estimated volume, while a value of $F_1 = 1$ indicates perfect agreement. In figures 6(a) and (b) the results of the proposed and SP method were connected for each image, which shows the tendency of the proposed method to climb towards the upper-right corner, which obviously corresponds to higher F_1 values. Table I shows averaged results for each of the evaluation metrics on the whole dataset, the bold ones being the best in each case.

TABLE I
AVERAGED COMPARISON RESULTS

| | F_1 | Precision | Recall | Hausdorff | Average dist |
|--------------|-------------|-------------|-------------|-------------|--------------|
| GDHB | 0.88 | 0.85 | 0.92 | 2.51 | 0.66 |
| SP | 0.79 | 0.69 | 0.94 | 5.63 | 1.46 |
| SP (3-seeds) | 0.76 | 0.68 | 0.89 | 5.82 | 1.53 |

As can be seen, the evaluation metrics report the superiority of the proposed method. The only exception is image #7 where the Hausdorff and the undirected averaged distance report slightly better results, in terms of actual and estimated boundary distances, but the other metrics report similar performance. In every testing case, the use of GDHB map, diminishes leakage and constraints the contour in the bounded area that describes. Shape prior methodology is not able to segment all

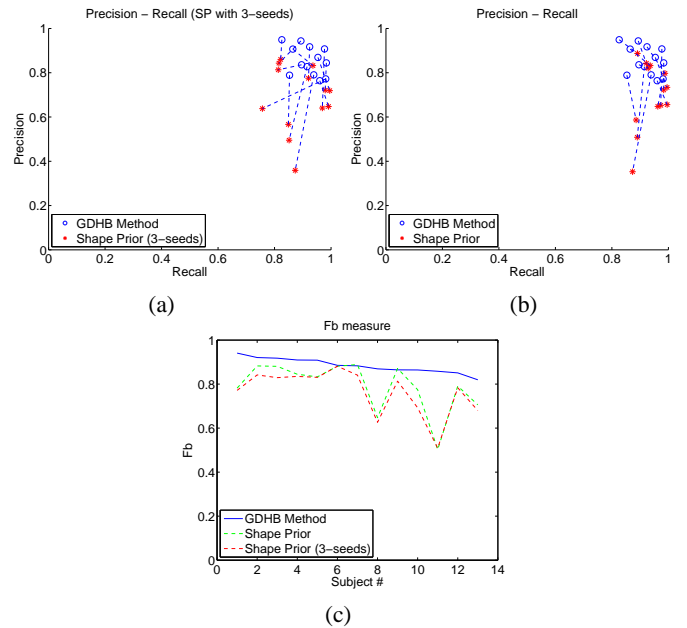


Fig. 6. Comparisons based on Precision vs Recall diagrams and the F_1 /Dice coefficient. In (a) and (b) results of the two methods are connected with dashed lines to show the improvement the proposed method achieved.

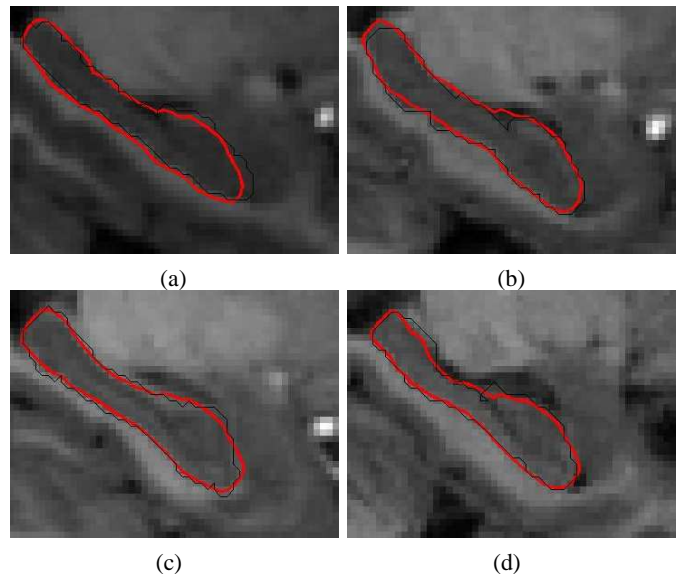


Fig. 7. Segmentation results of the proposed method on the four images with indexes 11, 5, 1 and 4 respectively. The thin black contour depicts the ground truth, while the red one is the outcome of the proposed method. Note the difference in segmentation quality between the proposed method in (b) and the SP method in 2(b) which are on the same MR image #5.

MR images with satisfying results, especially when initialized with the three seeds. Moreover, through experimentation, it became evident that the proposed method does not require fine tuning of the parameters, contrary with the SP case, where it was hard to find a set of parameters that satisfy the whole set. Furthermore, the results also show the contribution of the hippocampus spatial distribution map in the initialization procedure, since this utilization yields overall better accuracy and lower distance errors.

The segmentation procedure lasts no more than 10 seconds

for our experiments, in a quad-core PC, 2.8 GHz with 3.5 GB of RAM.

V. CONCLUSION

The proposed method utilizes two terms in the evolution process; the regional intensity based Chan-Vese model and a prior knowledge term. Previous works that incorporated prior knowledge into their models have succeeded efficient segmentations. However, the way that these two terms are combined is based on global weight multiplicative factors, which act globally on both terms, which contradicts with the nature of the hippocampus boundary. Our work proposes the use of the GDHB map in order to estimate locally, how much the image data are to be trusted or not. GDHB acts as a multiplicative weighting map to both terms, which mimics, even more, the way human experts perform the procedure. Early results verify this argument.

ACKNOWLEDGEMENTS

The authors would like to thank the OASIS team for providing us with their dataset and give special thanks to Angelos Baltatzidis M.D., Radiologist for building the training set by performing the manual segmentations of hippocampus and amygdala.

REFERENCES

- [1] X. Bresson, P. Vandergheynst and J.P. Thiran, "A variational Model for object segmentation using boundary information and shape prior driven by the Mumford-Shah functional", *International Journal of Computer Vision*, 68(2), 145-162, 2006.
- [2] V. Caselles, R. Kimmel, G. Sapiro, "Geodesic active contours", *International Journal of Computer Vision*, 22(1), 61-79, 1997.
- [3] T. Chan, W. Zhu, "Level set based shape prior segmentation", in *Proc. IEEE Conf. Comp. Vision Pattern Recognition*, 1164 - 1170, vol.2, 2005.
- [4] T. Chan and L. Vese, "Active contours without edges", *IEEE Trans. Image Processing*, vol. 10, pp. 266277, 2001.
- [5] J.G. Csernansky, L. Wang, D. Jones, D. Rastori-Cruz, J.A. Posener, G. Heydenbrand, J.P. Miller, M.I. Miller, "Hippocampal Deformities in Schizophrenia characterized by high dimensional brain mapping", *American Journal of Psychiatry*, 159:12, 2002.
- [6] C. Davatzikos, X. Tao, and D. Shen, "Hierarchical active shape models, using the wavelet transform", *IEEE Trans. on Medical Imaging*, vol 22, no 3, 2003.
- [7] J. M. Leventon, E. Grimson, and O. Faugeras, "Statistical shape influence in geodesic active contours", in *Proc. IEEE Conf. Comp. Vision Pattern Recognition*, vol. 1, pp. 316323, 2000.
- [8] C. Li, C. Xu, C. Gui, and M. D. Fox, "Distance Regularized Level Set Evolution and its Application to Image Segmentation", *IEEE Trans. Image Processing*, vol. 19 (12), 2010.
- [9] S. Loncaric, "A survey of shape analysis techniques", *Pattern Recognition*, vol.31, no 8, pp.938-1001, 1998.
- [10] D.S. Marcus, T.H. Wang, J. Parker, J.G. Csernansky, J.C. Morris, and R.L. Buckner, "Open Access Series of Imaging Studies (OASIS): Cross-Sectional MRI Data in Young, Middle Aged, Nondemented, and Demented Older Adults", *Journal of Cognitive Neuroscience*, 19, 1498-1507.
- [11] D. Martin, C. Fowlkes, and J. Malik, "Learning to detect natural image boundaries using local brightness, color and texture cues", *IEEE Trans. on Pattern Analysis and Machine Intelligence*, vol26, no 5, pp.530-549, 2004.
- [12] D. Mumford, J. Shah, "Optimal approximation by piecewise smooth function and associated variational problems", *Communication on Pure and Applied Mathematics* 42, pp. 577685,1989.
- [13] M.E. Shenton, G. Gerig, R.W. McCarley, G. Szekely, and R. Kikinis, "Amygdala-hippocampal shape differences in schizophrenia: the application of 3D shape models to volumetric MR data", *Psychiatry Research Neuroimaging*, 115, 15-35, 2002.
- [14] J. Talairach, P Tournoux, "Co-planar stereotaxic atlas of the human brain: An approach to medical cerebral imaging", New York: Thieme, 1988.
- [15] B. Vemuri and Y. Chen, "Joint image registration and segmentation", *Geometric level set methods in Imaging, Vision and Graphics*, Springer, pp. 251-269, 2003.
- [16] J. Yang, L.H. Staib and J.S. Duncan, "Neighbor-Constrained Segmentation with Level Set Based 3D Deformable Models", *IEEE Trans. on Medical Imaging*, vol. 23(8), 2004.
- [17] K. Zhang, L. Zhang, H. Song, and W. Zhou, "Active contours with selective local or global segmentation: A new formulation and level set method", *Image Vision Computing*, 28(4): 668-676, 2010.
- [18] Y. Zhang, B.J. Matuszewski, L.K. Shark, C.J. Moore, "Medical image segmentation using new hybrid level set method", *IEEE Int. Conf. on Biomedical Visualization*, 2008.